Tellus SERIES A DYNAMIC METEOROLOGY AND OCEANOGRAPHY
PUBLISHED BY THE INTERNATIONAL METEOROLOGICAL INSTITUTE IN STOCKHOLM

Tellus (2010), 62A, 698–705

TELLUS

Non-stationary drainage flows and motions in the cold pool

By L. MAHRT,[1]* SCOTT RICHARDSON,[2] NELSON SEAMAN[2] and DAVID STAUFFER[2],
[1]*COAS, Oregon State University, Corvallis, OR 97331, USA;* [2]*Department of Meteorology, Pennsylvania State University, University Park, PA 16802, USA*

(Manuscript received 25 January 2010; in final form 24 June 2010)

ABSTRACT

The initial formation of drainage flows and subsequent interaction with the cold pool are examined by contrasting winds measured with 2-sonic anemometers at three stations along a gentle slope for a 45-d observational period in late summer and early fall. On clear nights with weak winds, the station at the bottom of the slope experiences downslope flow only at the beginning of the evening, which quickly yields to light winds of variable direction after formation of a cold pool on the valley floor. A second station, several hundred metres up the slope, experiences drainage flow in the first part of the evening, which diminishes and yields to light and variable winds in the middle of the night as the influence of the cold pool deepens and engulfs the station. Drainage flow continues throughout the night at the third station located still farther up the slope and above the cold pool throughout the night. The interplay between the drainage flow, large-scale flow and submeso motions leads to frequent large shifts of wind direction. The character of the wind-direction variability differs substantially between the three stations. Large remaining uncertainties are noted.

1. Introduction

Most land surfaces, even those with very weak slopes, experience nocturnal drainage flows under clear skies and weak synoptic flow (e.g. Caughey et al., 1979; Mahrt and Larsen, 1990; Aubinet, 2008; Whiteman and Zhong, 2008). In addition to clear skies, drainage flows require large-scale winds to be weaker than a threshold value, sometimes posed in terms of a Froude number and/or Richardson number (e.g. Holden et al., 2000; LeMone et al., 2003). Well-developed cold air drainage has been studied extensively from observations, both above and within canopies (e.g. Sun et al., 2007; Aubinet, 2008 and references therein). The dynamics of earlier treatments of drainage flows are categorized in Mahrt (1982) for stationary flow over a constant slope with simple friction. Grisogono and Oerlemans (2001) provide more complete coupling between the temperature and wind field. The above studies often neglect the pressure gradient term.

Actual drainage flows are generally non-stationary to some degree and are often intermittent. The intermittency is sometimes attributed to interactions between mixing, mean shear and stratification of the drainage flow (e.g. Doran and Horst, 1981). Stone and Hoard (1989) and Poulos et al. (2007) demonstrate the modulation of drainage flows by wave motions. Often, drainage flows at a given point arrive as a microfront with a wind-direction shift and sudden temperature decrease (Blumen et al., 1999). Papadopoulos and Helmis (1999) find that drainage flow at the bottom of a given slope can be generated gradually by local cooling or arrive as a sharp advected microfront with sudden wind-direction change and sharp temperature decrease. The occurrence of these two contrasting regimes depends on the distribution of cooling along the slope, stratification at the bottom of the slope and the ambient wind speed and direction. Figure 3 of Monti et al. (2002) reveals the onset of drainage flow with characteristics of both of these two asymptotic regimes, in which a sharp wind-direction change occurs, but the enhanced temperature decrease is spread over 10 min or more. In other cases, the drainage flow in their study arrives as a sudden wind shift with minimal initial temperature decrease followed by a steady temperature decrease.

Cold pools begin to form in depressions, valleys and basins in the early evening transition after the net surface radiation becomes negative. Cold air drainage down sloping terrain often flows over the even colder air in the valley, as observed by Heywood (1933) and Yoshino (1984). Cold pools occur on a wide variety of scales (Blumen, 1984; Neff and King, 1989; Whiteman et al., 1999; Whiteman, 2000; Whiteman et al., 2001; Clements et al., 2003; Cuxart et al., 2007; de Araújo et al., 2008; Yao and Zhong, 2009) and have been predicted to form in even

*Corresponding author.
e-mail: mahrt@nwra.com
DOI: 10.1111/j.1600-0870.2010.00473.x

shallow valleys (Vosper and Brown, 2008; Bodine et al., 2009; Shapiro et al., 2009). Cold pool formation may be encouraged when the basin/valley outflow is retarded by opposing ambient flow (LeMone et al., 2003). The formation of cold pools in deep valleys has been numerically examined by Anquetin et al. (1998) using the model 'Submeso'.

In this study, 'submeso' will roughly refer to all horizontal scales between turbulence scales (thought to be generally less than 20 m in the thin drainage flows) and the smallest meso gamma scale, the latter usually considered to be 2 km (Orlanski, 1975). These motions include gravity waves, microfronts and numerous other more complex signatures. While some aspects of cold pool formation and well-defined drainage flows are understood for idealized situations, the non-stationary interactions between the two systems are poorly understood, as is the influence of common external submeso motions on such flows. As a beginning, this short study documents the diurnal variation and smaller-scale non-stationarity of the flow on the slope and in the cold pool using data from three stations of a new micronetwork in moderately complex terrain.

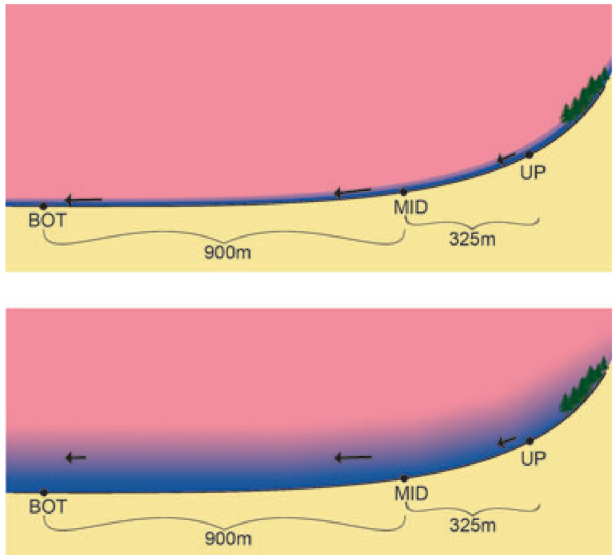

Fig. 1. A schematic cross section of the three stations on the northwest-facing slope of Tussey Ridge. The upper panel depicts the inferred flow during the early evening while the lower panel depicts the flow in the middle of the night. Blue indicates colder temperatures.

2. Data

Data analysed in this study were obtained from the Rock Springs Network near State College, PA, USA (40° 43 N, 77° 56 W) during the period 31 August (DOY 244) until 16 October (DOY 290) 2008. The stations are located on the lower slope of Tussey Ridge, where it meets the Nittany Valley, which is primarily covered by grassland. The upper 2/3 of the slope above the network is forested primarily with oak and other deciduous trees, and some evergreens (pine, fir and hemlock).

The upslope station (UP in Fig. 1) is at an elevation of about 50 m above the valley floor and just 15 m downslope from the edge of the forest. The midslope station (MID) is 325 m down the slope from station UP with a 30-m decrease of surface elevation, corresponding to a slope of approximately 9% (5.3°) between MID and UP. A third station (BOT) is located 900 m farther down the slope, nearly at the valley floor. The 20-m decrease of surface elevation between MID and BOT corresponds to a slope of 2.5% (1.3°) Due to the shallow depth of the drainage flows in this area, wind was measured at 2 m above the local surface at each of these stations using WS425 2D Väisälä sonic anemometers. Raw data were recorded at 1 Hz and averaged over 1-min intervals.

Temperature, T, was measured by Väisälä T107 temperature probes at 1 Hz and averaged to 1-min intervals. In addition, a network of 20 Hobo thermistors (Whiteman et al., 2000; Nakamura and Mahrt, 2005) were deployed in the forest subcanopy on the higher slope above UP.

For simplicity, we define a local potential temperature, θ_L, in terms of the adiabatic lapse rate, $\Gamma_D \approx 0.01$ K m^{-1}, such that

$$\theta_L \equiv T + \Gamma_D \delta z, \quad (1)$$

where δz is the relative elevation above the bottom station. The difference between this expression and the usual definition of potential temperature in terms of pressure for the small range of z is smaller than the measurement uncertainty. Unless otherwise stated, analyses will be limited to the nocturnal period between 2100 and 0500 LST.

3. Contrasting winds along the slope

3.1. General

The data set includes 40 nights of data. Twenty-four of the nights reveal a systematic evolution of the slope flow and cold pool formation, including the first 4 d of the experiment, which are studied in more detail below. Eight nights revealed no drainage flow/cold pool formation. These nights exhibited restricted or no nocturnal cooling. Eight additional nights revealed some elements of formation of drainage flow/cold pool formation, but were less defined compared to the primary case study period.

The following analyses the 33 nights of data where the observations were available at all three stations. Frequency distributions for wind speeds at the three slope stations (Fig. 2) show that nocturnal flow for this late summer to early autumn field program is often quite weak in the sheltered environment of the Nittany Valley. Nocturnal winds greater than 2 ms^{-1} are uncommon and generally are due to stronger-than-normal synoptic pressure gradients. However, there are significant differences between the weak winds at these three sites. Extremely weak winds (speed $<$0.5 ms^{-1}) are the most common at the bottom station (Fig. 2, black) due to early formation of the nocturnal cold pool. Speeds

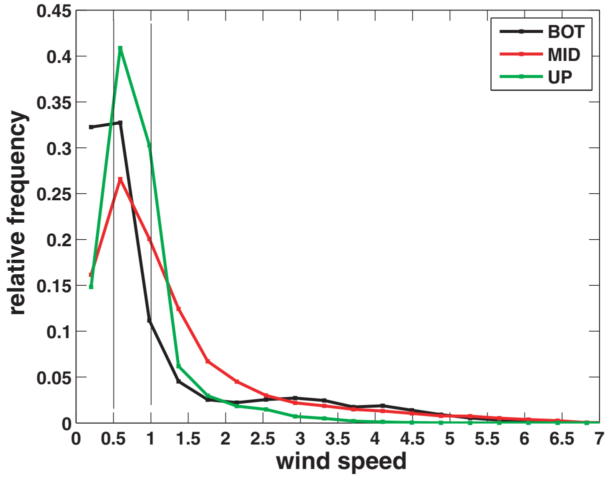

Fig. 2. The 45-d relative frequency distribution of the magnitude of the nocturnal 1-min vector-averaged wind speeds for 31 August–16 October 2008. Thin vertical lines are for reference only.

of 1 ms^{-1} or more occur here least often amongst the three sites. Winds at the upslope station (Fig. 2, red) are associated with weak drainage flow, peaking at about 0.5 ms^{-1}. The winds at the bottom and upslope stations are less than 1 ms^{-1} about 75% of the time. The frequency of such very weak winds is less at the midslope station (Fig. 2, green), partly due to acceleration of the drainage flow between stations UP and MID.

The frequency distribution of the 1-min wind directions at the upslope station (Fig. 3) shows a major peak at 130°, in approximate alignment with the northwest-facing local terrain slope. The frequency distribution for the midslope station also shows a significant peak at 130°, but is less pronounced than at the upslope station and includes more frequent southerly flow

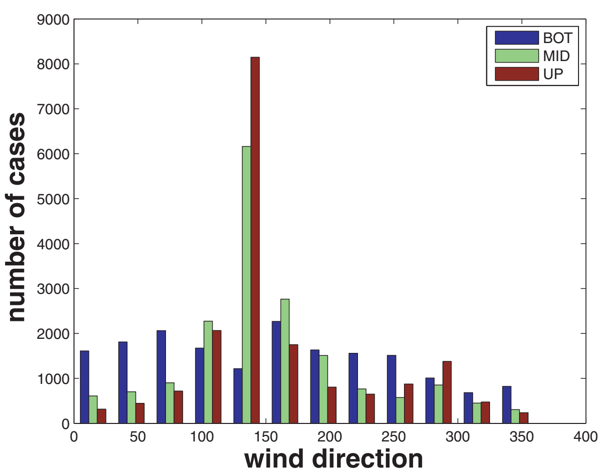

Fig. 3. The 45-d frequency histogram of the nocturnal wind directions for 30° direction intervals based on 1-min vector-averaged winds for 31 August–16 October 2008.

compared to the upslope station. The bottom station experiences significant occurrences from all direction sectors. The lack of directional preference in the cold pool is consistent with the very weak downvalley slope at this station and the influence of submeso motions. Due to a col in the valley floor near the bottom station, the downvalley slope is near zero or less than 1% downward toward the northeast for a distance of about 3 km downvalley from the network, after which the slope gradually increases to values greater than 1%.

3.2. Case study

We now focus on a 4-d period of fair weather at the beginning of the data set from 31 August to 4 September, 2008. During this period, the network lies under a broad slow-moving upper-level ridge, which finally moves eastward off the east coast of the United States on 5 September, terminating the case study period. Daytime 850 hPa flow for the period is mostly west–northwesterly at about 5 ms^{-1}.

The nocturnal winds at the upslope station are consistently southeasterly downslope flow (upper panel, Fig. 4) and on the order of 1 ms^{-1} or less. This downslope flow weakens only slightly during the course of each night. The southeasterly downslope flow at the midslope station at the beginning of the night (middle panel, Fig. 4) is about twice as strong as that at the upper station, but weakens significantly and almost vanishes after midnight, presumably due to the influence of the deepening cold pool. Limited temperature measurements on a nearby 47-m tower (not shown) support this hypothesis, although the cold pool does not have a distinct top. After the early evening transition, the site at the bottom of the slope (Fig. 4, bottom panel) is apparently in the cold pool all night and experiences very weak winds with no obvious directional dependence.

3.3. Early evening drainage formation

The evening transition and development of drainage flow is somewhat different each night, but certain features are common to all four nights and most other clear nights throughout the 45-d observational period. Figure 5 displays winds and temperatures for a 120-min period during the evening transition after 1645 LST on 31 August, the first night of the fair-weather case study. At the upslope station, (upper panel, Fig. 5), drainage flow from the south–southeast begins about 5 min into the Fig. at 1650 LST. Gradual cooling commences at the upslope station with the onset of the drainage flow. The drainage flow arrives more abruptly at the midslope station (middle panel, Fig. 5), with a larger temperature decrease and a lag of almost 40 min, compared to the upslope station. The long time delay may indicate that the drainage flow creeping out of the forest subcanopy dissipates during this early period before reaching the MID station, or, the drainage flow initially arrives as a thin flow underneath the 2-m measurement. While the drainage flow at the upslope

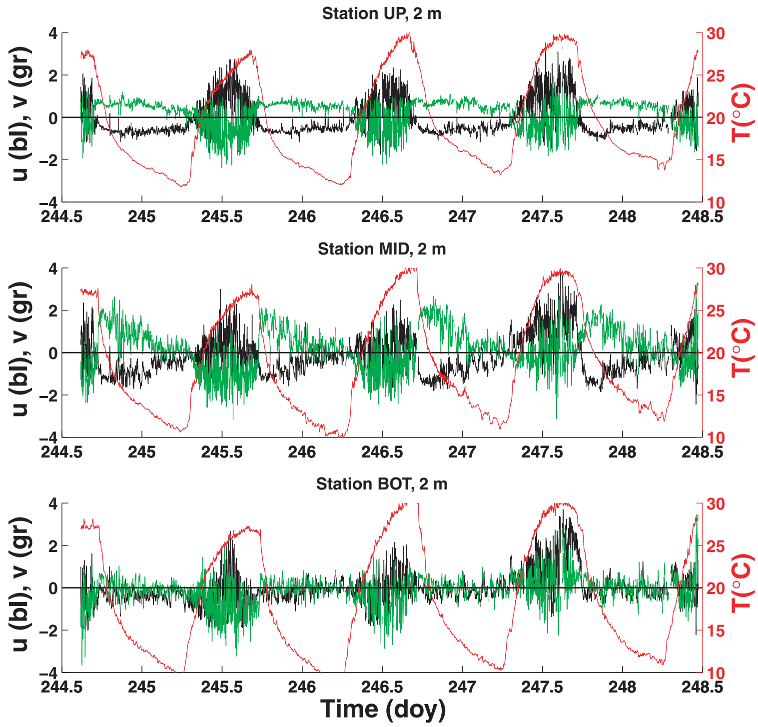

Fig. 4. Horizontal wind components (ms^{-1}) and temperature (K) during the 4-d case-study period, 31 August–4 September 2008. Time shown in Julian days.

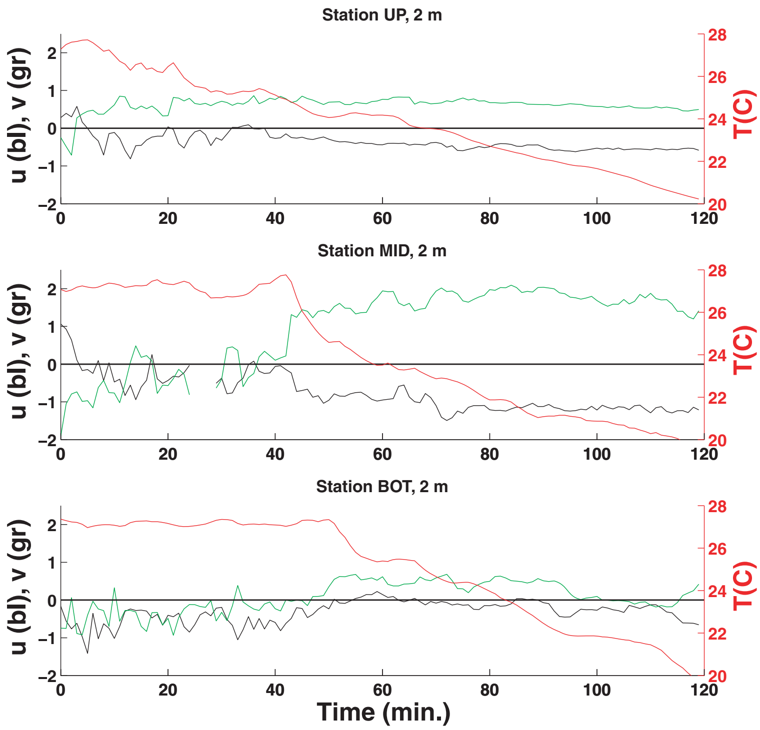

Fig. 5. Onset of drainage flow on 31 August for the three stations for the transition period, as a function of minutes after 1645 LST, when the cooling and downslope flow first start at the upper station. Thin vertical lines indicate approximate onset of drainage flow. Sunset is approximately 1845 LST, the end of this plot.

station is about 1 ms^{-1}, the drainage flow at the midslope station consistently exceeds 1 ms^{-1}. The small surface roughness of the grass field and stronger surface cooling compared to under the forest subcanopy, contribute to downslope acceleration over the grass field. While the downslope flow at the upslope station arrives with about the same temperature as the upwind subcanopy, the temperature cools by several degrees over the field between the upslope and midslope stations (Fig. 6), due to less

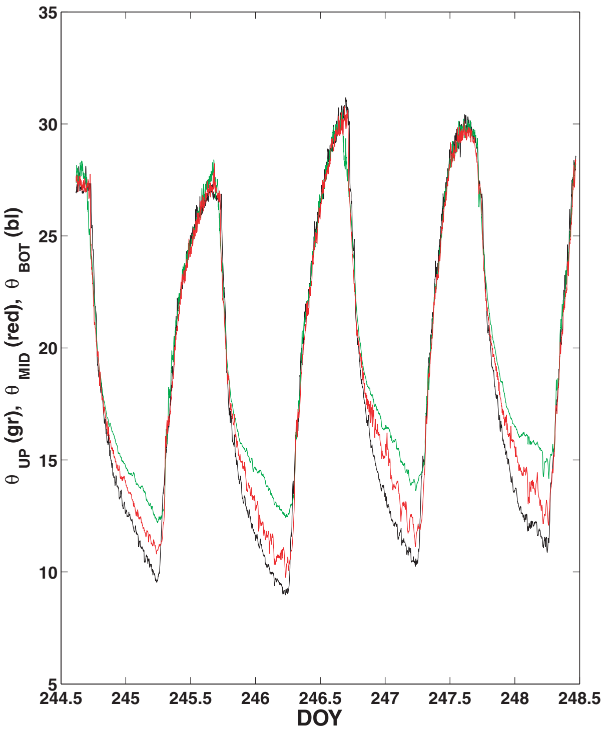

Fig. 6. Local potential temperature for the 4-d case study for the three stations. Time shown in Julian days.

mixing (smaller roughness) and no overstorey (less downward longwave radiation).

At the bottom station during this period, the weak drainage flow begins with a sudden 2 °C temperature decrease about 10 min after its abrupt arrival at the midslope station. This time difference between the two stations corresponds to a propagation speed on the order of 1.5 ms^{-1}, which is the same order of magnitude as the downslope flow. More definite conclusions are not possible since the stations are generally not on the same trajectory, partly due to short-term variations of wind direction on submeso time scales.

The weak drainage flow at the bottom of the slope (right edge of Fig. 5, bottom panel) survives for less than an hour before yielding to weak winds of variable direction driven by submeso motions on time scales of minutes to tens of minutes (Fig. 4, bottom panel). While the arrival of the drainage flow begins the significant cooling at the bottom of the slope, the temperature decrease is small compared to the total cooling during the night. This result and the eventual formation of a much deeper cold pool suggest that the early evening arrival of the drainage flow does not contribute significantly to the total heat budget of the cold pool, as also observed by Bodine et al. (2009).

The drainage flow at the upslope station (adjacent the forest) begins almost 2 h before sunset, probably due to the more complete shading of the subcanopy by the overstorey at low sun angles on this northwest facing slope. The drainage flow arrives at the mid slope and bottom stations a little more than an hour before sunset. Reversal to negative net radiation occurs earlier than the sunset.

The sudden temperature decrease observed with the onset of drainage flow is a local phenomenon superimposed upon a more general exponential-like decrease of temperature during the course of the night (de Wekkerand Whiteman, 2006). On some nights, the onset of downslope flow is not accompanied by the usual sudden decrease of temperature, but only by a sudden increase of the cooling rate. That is, the downslope flow marks the beginning of the exponential decrease of temperature with time, so that the drainage flow corresponds to a sudden increase in cooling rate rather than a sudden decrease of temperature. Several nights experienced a short warm event just after the arrival of drainage flow, consistent with an overturning eddy at the leading edge of the drainage flow (e.g., Sun et al., 2002).

After the evening transition, strong stratification develops along the slope. The potential temperature decreases down the slope by as much as 4 °C over an elevation difference of 50 m due to more rapid cooling in the valley compared to along the slope (Fig. 6). Large fluctuations of temperature at the midslope station occur on three of the four nights after the drainage flow has weakened or vanished in the middle of the night (Fig. 6), perhaps reflecting undulations in the depth of the cold pool.

The pattern of weak winds and variable wind direction between the daytime west–northwesterly flow (Fig. 4) and the onset of drainage flow defines an 'early evening calm' period (left-hand side of Fig. 5), although the ensuing drainage flow is significantly stronger only at the midslope station. The existence and nature of this early evening calm before the development of the nocturnal circulations varies between nights. This calm period has been reported by Acevedo and Fitzjarrald (2001) and can be seen in fig. 8 of Mahrt et al. (2001). During this period, models can overpredict the surface momentum flux (Edwards et al., 2006), which may not be in approximate equilibrium with the rapidly evolving mean flow (Grant, 1997).

4. Wind direction variability

Unpredictable shifts of wind direction due to submeso winds and intermittent drainage flows on time scales of minutes or tens of minutes can be especially problematic for forecasting the dispersion of contaminants. Here, we use three measures of variability of the wind direction within 1-h periods, based on the 1-min vector-average winds. The first measure is the maximum of the absolute value of the wind-direction change during the hour, computed using centred differences. That is, the time change of wind direction at minute i is the difference between the wind direction at minute $i + 1$ and minute $i - 1$. As the second measure of wind-direction variability, we compute the standard deviation of the centre-differenced minute-to-minute changes within the 1-h period. Computation of such wind-direction statistics is

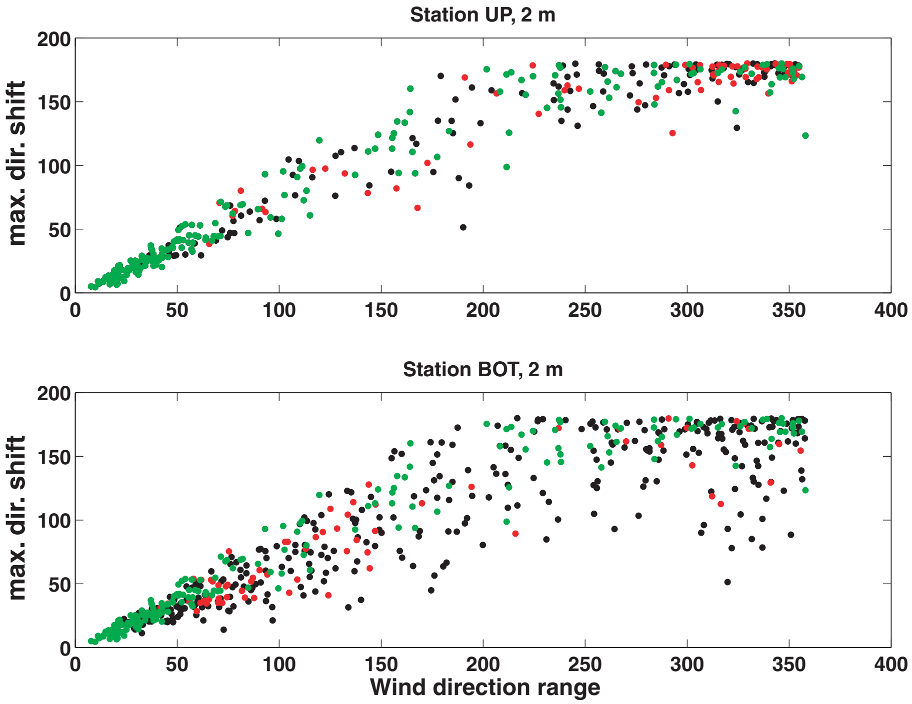

Fig. 7. Maximum 1-min wind-direction shift within a given 1-h record as a function of the hourly range of wind direction at the upper (upper panel) and lower (lower panel) stations. Green dots correspond to nocturnal cases with southeasterly flow at the upper station (normally drainage flow) while black dots represent hours with other wind directions at the upper station. More strict criteria for drainage flow separate the points more clearly, but reduces the number of cases of drainage flow. The red dots define the early-evening transition from 1800 to 2000 LST.

complicated by the cyclic nature of wind direction and here requires iteration, as in Mahrt (2008). The total range of the 1-min wind direction within each 1-h record serves as the third measure of the wind-direction variability. Since the range is defined by the maximum positive and negative deviations from the mean wind, the range can approach 360°. These three measures of variability were computed based on all of the nocturnal hours (2000–0500 LST) for the 33 nights with data at all three stations.

The standard deviation of the wind direction (not shown) exhibits the usual inverse relationship with the wind speed (e.g. Davies and Thomson, 1999). The maximum wind-direction shift during a 1-h period is relatively well correlated with the wind-direction range (Fig. 7) with some significant exceptions. The bottom station includes cases of large wind-direction change approaching 360° with rather modest maximum wind-direction shifts of less than 100° (right-hand side of bottom panel). Although these cases are not numerous, they best fit the concept of gentle meandering of the wind direction. For these cases, the large wind-direction range is an accumulation of small minute-to-minute wind-direction changes during the course of the hour as would occur with gradual change of the wind direction over a period of time. However, most of the hours with large wind-direction change at the bottom station also include large minute-to-minute wind-direction shifts exceeding 100° within the hour. Cases of small wind-direction variability at the bottom station (left-hand side of bottom panel) correspond to substantial synoptic flow, often from the southwest.

In contrast to the bottom station, large wind-direction range occurs at the upper station only with large maximum wind-direction shift. These large wind-direction shifts generally occur when the drainage flow is intermittent on nights where the synoptic flow is more significant or the cooling may be weaker compared to the 4-d case study period. For this case-study period (Fig. 4), the wind-direction variability is small at the upper station, corresponding to the lower left-hand corner of the upper panel (Fig. 7). However, even brief disruption of the drainage flow can lead to large wind-direction change.

During the early evening transition (red dots), the wind direction varies more at the upper station (more red points in the upper right-hand corner of the upper panel) compared to the bottom station. The drainage flow in the early evening is often only intermittent at the upper station (large wind-direction variability), whereas the drainage flow does not penetrate to the bottom station when the wind remains coupled to the ambient flow during the early transition period (small direction variability).

To contrast periods with drainage flow with periods without drainage flow, hours with mean wind vector from the southeast quadrant at the upper station are plotted with green dots for both stations in Fig. 7, whereas the remaining periods are plotted as black dots. For the periods of drainage flow, the wind-direction variability at the upper station tends to be smaller than for periods without mean drainage flow. This leads to a large cluster of green points in the lower left-hand corner, representing semi-stationary drainage flows. Semi-stationary drainage flow at the upper station corresponds to greater maximum wind-direction shifts at the bottom station compared to other cases at the bottom station (compare green and black dots in the lower panel). These large wind-direction shifts appear to be more related to general submeso motions in very weak-wind conditions rather than pulses of drainage flow penetrating the cold pool. That is, weak large-scale flow independently leads to drainage flows on the slope and large wind-direction changes in the cold pool.

Considering all of the nights collectively, a substantial fraction of hourly records for all three sites exhibits large maximum wind-direction shift and/or large wind-direction range. During these common periods, the release of contaminants near the surface would disperse in widely different directions even within a 1-h period.

5. Conclusions

The above study briefly documents the formation of drainage flow and its termination at the bottom of the slope. The drainage flow penetrates to the valley floor mainly at the beginning of the evening, sometimes preceded by an 'early evening calm'. As colder air collects in the valley cold pool, the drainage flow no longer penetrates to the bottom of the slope. In the early part of the evening, the flow accelerates over the grass-covered lower part of the slope fed by subcanopy flow from the upper part of the slope. This acceleration diminishes as the cold pool thickens and occupies more of the grass-covered slope.

Interaction of the drainage flow with the cold pool and submeso motions leads to unpredictable large changes of wind direction, particularly within the cold pool. Direction changes higher on the slope often reveal interplay between the large-scale flow and drainage flow. These common, but more complex scenarios, have been ignored in the literature and require more attention.

6. Acknowledgments

The extensive and important comments of the reviewers are gratefully acknowledged. This material is based upon work supported by DTRA grants HDTRA1-10-1-0033 and W911NF-06-1-0439 and ARO Contract W911FN05C0067.

References

Acevedo, O. C. and Fitzjarrald, D. R. 2001. The early evening surface-layer transition: temporal and spatial variability. *J. Atmos. Sci.* **58**, 2650–2667.

Anquetin, S., Guilbaud, C. and Chollet, J. P. 1998. The formation and destruction of inversion layers within a deep valley. *J. Appl. Meteorol.* **37**, 1547–1560.

Aubinet, M. 2008. Eddy covariance CO_2 flux measurements in the nocturnal conditions: an analysis problem. *Ecol. Appl.* **18**, 1368–1378.

Blumen, W. 1984. An observational study of instability and turbulence in nighttime drainage winds. *Boundary-Layer Meteorol.* **28**, 245–269.

Blumen, W., Grossman, R. and Piper, M. 1999. Analysis of heat budget, dissipation and frontogenesis in a shallow density current. *Boundary-Layer Meteorol.* **91**, 281–306.

Bodine, D., Klein, P., Arms, S. and Shapiro, A. 2009. Variability of surface air temperature over gently sloped terrain. *J. Appl. Meteorol.* **48**, 1117–1141.

Caughey, S. J., Wyngaard, J. C. and Kaimal, J. C. 1979. Turbulence in the evolving stable boundary layer. *J. Atmos. Sci.* **36**, 1041–1052.

Clements, C. B., Whiteman, C. D. and Horel, J. D. 2003. Cold-air-pool structure and evolution in a mountain basin: Peter Sinks, Utah. *J. Appl. Meteorol.* **42**, 752–768.

Cuxart, J., Jiménez, M. A. and Martínez, D. 2007. Nocturnal mesobeta basin and katabatic flows on a midlatitude island. *Mon. Wea. Rev.* **135**, 918–932.

Davies, B. M. and Thomson, D. J. 1999. Comparisons of some parameterizations of wind direction variability with observations. *Atmos. Environ.* **33**, 4909–4917.

de Araújo, A., Kruijt, B., Antonio, A., Nobre, A., Dolman, J. and co-authors. 2008. Nocturnal accumulation of CO_2 underneath a tropical forest canopy along a topographical gradient. *Ecol. Appl.* **18**, 1406–1419.

de Wekker, S. and Whiteman, C. D. 2006. The time scale of nocturnal boundary layer cooling in valleys and basins and over plains. *J. Appl. Meteorol. Clim.* **45**, 813–820.

Doran, J. C. and Horst, T. W. 1981. Velocity and temperature oscillations in drainage winds. *J. Appl. Meteorol.* **20**, 360–364.

Edwards, J. M., Beare, R. J. and Lapworth, A. J. 2006. Simulation of the observed evening transition and nocturnal boundary layers: single-column modelling. *Quart. J. Roy. Meteorol. Soc.* **132**, 61–80.

Grant, J. L. M. 1997. An observational study of the evening transition boundary-layer. *Quart. J. Roy. Meteorol. Soc.* **123**, 657–677.

Grisogono, B. and Oerlemans, J. 2001. Katabatic flow: analytic solution for gradually varying eddy diffusivities. *J. Atmos. Sci.* **58**, 3349–3354.

Heywood, G. S. P. 1933. Katabatic winds in a valley. *Quart. J. Roy. Meteorol. Soc.* **59**, 43–57.

Holden, J. J., Derbyshire, S. H. and Belcher, S. E. 2000. Tethered balloon obser vations of the nocturnal stable boundary layer in a valley. *Boundary-Layer Meteorol.* **97**, 1–24.

LeMone, M. A., Kyoko, I., Grossman, R. and Rotach, M. 2003. Horizontal variability of 2-m temperature at night during CASES-97. *J. Atmos. Sci.* **60**, 2431–2450.

Mahrt, L. 1982. Momentum balance of gravity flows. *J. Atmos. Sci.* **39**, 2701–2711.

Mahrt, L. 2008. Mesoscale wind direction shifts in the stable boundary-layer. *Tellus* **60A**, 700–705.

Mahrt, L. and Larsen, S. 1990. Relation of slope winds to the ambient flow over gentle terrain. *Boundary-Layer Meteorol.* **53**, 93–102.

Mahrt, L., Vickers, D., Nakamura, R., Sun, J., Burns, S. and co-authors. 2001. Shallow drainage and gully flows. *Boundary-Layer Meteorol.* **101**, 243–260.

Monti, P., Fernando, H. J. S., Chan, W. C., Princevac, M., Kowalewski, T. A. and co-authors. 2002. Observations of flow and turbulence in the nocturnal boundary layer over a slope. *J. Atmos. Sci.* **59**, 2513–2534.

Nakamura, R. and Mahrt, L. 2005. Air temperature measurement errors in naturally ventilated radiation shields. *J. Atmos. Oceanic Tech.* **22**, 1046–1058.

Neff, W. and King, C. 1989. The accumulation and pooling of drainage flows in a large basin. *J. Appl. Meteorol.* **28**, 518–529.

Orlanski, I. 1975. A rational subdivision of scales for atmospheric processes. *Bull. Am. Meteorol. Soc.* **56**, 527–530.

Papadopoulos, K. H. and Helmis, C. G. 1999. Evening and morning transition of Katabatic flows. *Boundary-Layer Meteorol.* **92**, 195–227.

Poulos, G., Bossert, J., McKee, T. and Pielke, R. Sr. 2007. The interaction of katabatic flow and mountain waves. Part II: case study analysis and conceptual model. *J. Atmos. Sci.* **64**, 1875–1879.

Shapiro, A., Klein, P., Arms, S., Bodine, D. and Carney, M. 2009. The Lake Thunderbird Micronet Project. *Bull. Amer. Meteorol. Soc.* **90**, 811–823.

Stone, G. and Hoard, D. 1989. Low-frequency velocity and temperature fluctuations in katabatic valley flows. *J. Appl. Meteorol.* **28**, 477–488.

Sun, J., Burns, S. P., Lenschow, D. H., Banta, R., Newsom, R. and co-authors. 2002. Intermittent turbulence associated with a density current passage in the stable boundary layer. *Boundary-Layer Meteorol.* **105**, 199–219.

Sun, J., Burns, S., Delany, A., Oncley, S., Turnipseed, A. and co-authors. 2007. CO_2 transport over complex terrain. *Agric. For. Meteorol.* **145**, 1–21.

Vosper, S. B. and Brown, A. R. 2008. Numerical simulations of sheltering in valleys: the formation of nighttime cold-air pools. *Boundary-Layer Meteorol.* **27**, 429–448.

Whiteman, C. D. 2000. *Mountain Meteorology*. Oxford University Press, 355 pp.

Whiteman, C. D., Bian, X. and Zhong, S. 1999. Wintertime evolution of the temperature inversion in the Colorado Plateau Basin. *J. Appl. Meteorol.* **38**, 1103–1117.

Whiteman, C. D., Hubbe, J. and Shaw, W. 2000. Evaluation of an inexpensive temperature data logger for meteorological applications. *J. Atmos. Oceanic Tech.* **17**, 77–81.

Whiteman, C. D., Zhong, S., Shaw, W., Hubbe, J. and Bian, X. 2001. Cold Pools in the Columbia Basin. *Wea. Forecast* **16**, 432–447.

Whiteman, C. D. and Zhong, S. 2008. Downslope flows on a low-angle slope and their interactions with valley inversions. Part I: observations. *J. Appl. Meteorol. Clim.* **47**, 2023–2038.

Yao, W. and Zhong, S. 2009. Nocturnal temperature inversions in a small, enclosed basin and their relationship to ambient atmospheric conditions. *Meteorol. Atmos. Phys.* **103**, 195–210.

Yoshino, M. M. 1984. Thermal belt and cold air drainage on the mountain slope and cold air lake in the basin at quiet clear night. *Geophys. J.* **8**, 235–250.